

## Structural Investigation of an Adsorbate-Covered Surface with He Diffraction: Ni(110) + (1×2)H

K. H. Rieder and T. Engel

IBM Zurich Research Laboratory, 8803 Rüschlikon, Switzerland

(Received 9 April 1979)

This paper reports He diffraction from clean and hydrogen-saturated Ni(110) at 100 K. The clean surface can be described by a sinusoidal corrugation of amplitude 0.05 Å in the [001] azimuth. The hydrogen-saturated surface requires an additional corrugation of amplitude 0.23 Å on each second maximum of the basic corrugation. Possible adsorption structures consistent with this corrugation function are discussed.

Analysis of He diffraction data based on the corrugated hard-wall model<sup>1-4</sup> has yielded structural information on ionic crystals<sup>2,5</sup> and semiconductor surfaces.<sup>6</sup> Until now, this potentially powerful technique had not been applied to adsorbate-covered surfaces. In this Letter, we report the first diffraction study of a simple adsorbate system, Ni(110) + (1×2)H. The analysis of diffraction intensities of the clean and adsorbate-covered surface yields novel structural information.

The scattering experiments were carried out in an ultrahigh-vacuum system (base pressure  $5 \times 10^{-11}$  Torr) with low-energy electron diffraction (LEED), Auger electron spectrometry, and secondary-ion mass spectrometry capabilities. The wavelength,  $\lambda$ , of the He nozzle beam can be varied between 0.2 and 0.9 Å by heating and cool-

ing the nozzle. With the nozzle at 300 K ( $\lambda = 0.57$  Å), the velocity spread  $\Delta v/v$  is 8.5%, as evaluated from the width of the diffraction peaks. The instrumental resolution, which is determined by the beam diameter at the target and the detector aperture, is 1.7°. The quadrupole mass spectrometer is mounted on a goniometer, which allows inplane as well as out-of-plane detection.

The Ni(110) surface was prepared and cleaned with use of standard techniques. The crystalline perfection of the surface was confirmed by the high ratio of the specular to the incident He beam intensities, which varied between 0.2 and 0.5 for near-normal and near-grazing incidence. The scattering data presented here refer to a surface temperature of 100 K. The incident beam was parallel to the [001] azimuth [see Figs. 1(a) and 1(b)]. For the clean surface, strong (00), rela-

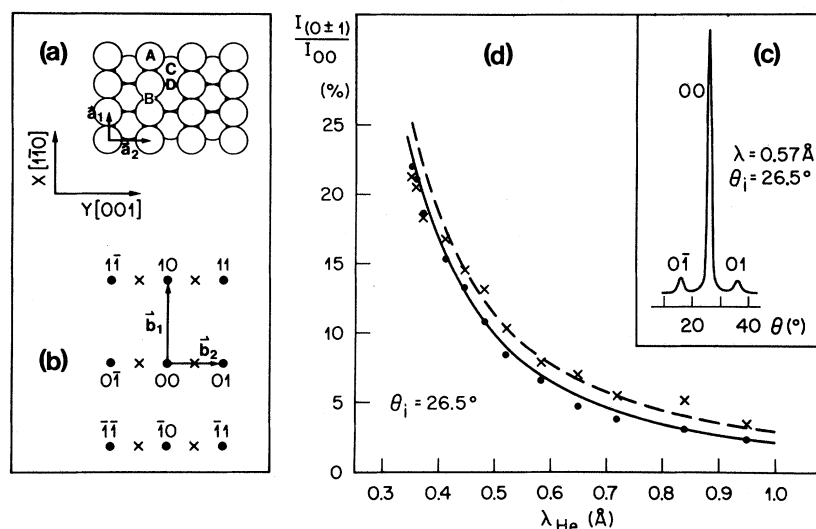


FIG. 1. (a) Hard-sphere model of the Ni(110) surface showing possible adsorption sites A, B, C, and D. (b) Reciprocal lattice corresponding to (a): Solid circles, diffraction beams of the substrate; Crosses, additional beams which appear upon H saturation. (c) He scattering spectrum for clean Ni(110). (d) He diffraction intensities of the (01) and (0 $\bar{1}$ ) beams relative to the (00) beam as a function of the wavelength  $\lambda$  for the clean Ni(100) surface. (01) beam: Solid circle, experiment; solid line, theory. (0 $\bar{1}$ ) beam: Crosses, experiment; dashed line, theory.

tively strong ( $0\bar{1}$ ) and (01), and very weak ( $0\bar{2}$ ) peaks were observed [Fig. 1(c)]. The intensity of the first-order beams relative to the specular are shown in Fig. 1(d) as a function of  $\lambda$ . Also shown in Fig. 1(d), are curves calculated with use of the hard-wall model within the eikonal approximation.<sup>1</sup> The diffraction probability for the beam corresponding to the reciprocal lattice vector  $\vec{G}$  is given by

$$P_G = \frac{k_{G_z} \left( \frac{\vec{k}_i \vec{q}_G}{\vec{k}_{G_z} \vec{q}_{G_z}} \right)^2 \frac{1}{A^2} \times \left| \int \exp\{i[\vec{G} \cdot \vec{R} - q_{G_z} \zeta(\vec{R})]\} d^2R \right|^2, \quad (1)$$

where  $\vec{k}_i$  and  $\vec{k}_G$  are the wave vectors of the incoming and diffracted beams and  $\vec{q}_G \equiv (\vec{G}, q_{G_z}) = \vec{k}_i - \vec{k}_G$  is the scattering vector;  $A$  denotes the area of the unit cell over which the integral is taken. The effect of the attractive well<sup>1</sup> has been neglected, as the well depth is very small for He on metals.<sup>7</sup> Furthermore, because of the low sample temperature as compared with the Debye temperature and the small  $\vec{G}$  vectors involved in diffraction, the angular variation of the intensities due to the Debye-Waller factor has been neglected. Since the (10) and ( $\bar{1}0$ ) beams were observed to be more than one order of magnitude weaker than the (01) and ( $0\bar{1}$ ) beams, the corrugation in the  $[1\bar{1}0]$  azimuth was neglected. The corrugation function was assumed to be

$$\zeta(R) = \frac{1}{2} \zeta_{0y} [1 - \cos(2\pi y/a)], \quad (2)$$

with  $a = |\vec{a}_2| = 3.52 \text{ \AA}$ . Excellent agreement with the observed intensity ratios of Fig. 1(d) was found for  $\zeta_{0y} = 0.055 \text{ \AA}$ . Somewhat poorer agreement was obtained for the dependence of the intensity ratios on  $\theta_i$  for  $\lambda = 0.57 \text{ \AA}$ . Using both data sets, we establish  $\zeta_{0y}$  to be  $0.05 \pm 0.01 \text{ \AA}$ .

Saturation of the Ni(110) surface with hydrogen [exposure 1.5 L (1 L =  $1 \mu\text{Torr sec}$ ) at 100 K] resulted in the formation of a  $(1 \times 2)$  structure as was confirmed with LEED. Figure 2 shows in-plane diffraction for various  $\theta_i$  for  $\lambda = 0.57 \text{ \AA}$ . Out-of-plane scattering revealed several ( $\pm 1n$ ) peaks with intensities more than 30 times smaller than the ( $0n$ ) peaks. Therefore, the corrugation along the  $[1\bar{1}0]$  azimuth was neglected as for the clean Ni surface. 30–50% of the incoming intensity is elastically scattered from the clean surface; for the H-covered surface, the corresponding value is 15–20%. The (00) beam is reduced by a factor of  $\sim 6$  upon adsorption.

Attempts to fit the spectra of Fig. 2 with a sinusoidal potential of periodicity  $d = 2a$  [see Eq. (2)]

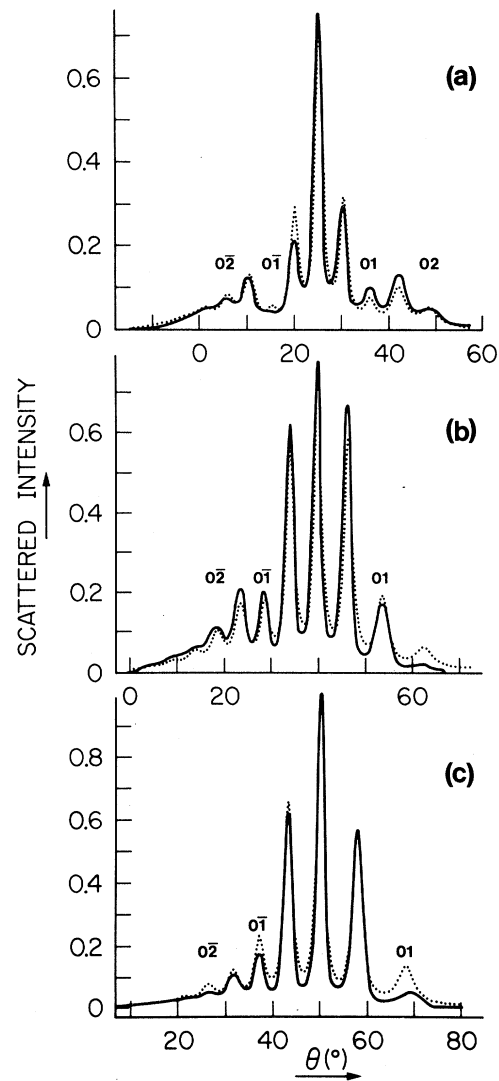


FIG. 2. He scattering intensities for hydrogen-saturated Ni(110) as a function of the scattering angle  $\theta$  for  $\theta_i$  values of (a)  $25.5^\circ$ , (b)  $40^\circ$ , and (c)  $50^\circ$ . (Solid lines indicate experiment; dotted lines, theory.) The experimental intensity of the (00) beam for  $\theta_i = 50^\circ$  was set equal to 1. The beam is incident parallel to the  $[001]$  azimuth [Figs. 1(a) and 1(b)].

gave no agreement with the observed intensities. In particular, the low intensities of the (01) and ( $0\bar{1}$ ) beams for small  $\theta_i$  [Fig. 2(a)] could not be reproduced. We therefore tried a corrugation function of the form

$$\zeta(R) = \frac{1}{2} \zeta_{0y} [1 \pm \cos(4\pi y/d)] + \delta_{1j} \zeta_{1y} \sin^2(2\pi y/d), \quad (3)$$

where  $\delta_{1j}$  is the Kronecker symbol and  $j = 1$  and 2 designate the first and second half of the elemen-

tary cell with length  $d=2a$ . The first term describes the corrugation of the substrate and the second allows for an extra contribution consistent with the double periodicity observed along the  $[001]$  azimuth. Agreement between theory and experiment could only be obtained with the minus sign in Eq. (3) and the best-fit parameters derived were  $\zeta_{0y}=0.04 \pm 0.01 \text{ \AA}$  and  $\zeta_{1y}=0.23 \pm 0.01 \text{ \AA}$ . Note that  $\zeta_{0y}$  is unchanged upon adsorption. The experimental and theoretical curves, normalized to the same height of the  $(00)$  peak, are compared in Fig. 2. Lorentzian peak shapes were assumed with half widths determined from the instrumental resolution and the velocity dispersion of the incoming beam. Fits of the same high quality have also been obtained for several other angles of incidence with use of the same corrugation parameters. The form of the corrugation was tested by replacing the  $\sin^2$  term in Eq. (3) by a  $\sin^4$  term. No satisfactory agreement with experiment was attained.

To obtain structural information from the corrugation functions, the hard wall must be associated with the position and size of each atom in the surface unit cell. If, as for  $\text{LiF}(100)^2$ , the hard wall were generated by a He atom rolling over a hard-sphere model of the clean  $\text{Ni}(110)$  surface,  $\zeta_{0y}$  should be  $0.56 \text{ \AA}$  rather than  $0.05 \text{ \AA}$ , as observed. This shows the smoothing influence of the electron spillover on the corrugation amplitude.  $\zeta_{0y}$  for  $\text{Ni}(110)$  is one third of the determined for  $\text{W}(112)$ , which has a similar structure with a larger spacing between the close-packed rows.<sup>8</sup> The relationship between the corrugation function and atomic positions is not as straightforward for metal surfaces as for ionic crystals; nevertheless, it is reasonable to associate maxima in the corrugation with atomic positions.

The following three models can describe the observed  $(1 \times 2)$  periodicity after hydrogen adsorption: (a) Adsorption occurs on the unreconstructed surface [see Fig. 1(a) for possible sites]; (b) upon adsorption alternate nickel rows are shifted perpendicular to the surface; and (c) upon adsorption the nickel rows are laterally displaced to form pairs [see Fig. 3(c)]. A principal difficulty in deciding between these models is due to the uncertainty in the hydrogen coverage which has been estimated variously as  $0.4$ ,<sup>9</sup>  $0.67$ ,<sup>10</sup> and  $1$  or  $2$ .<sup>11</sup>

Considering first model (a), it is easily seen that the coincidence of maxima of the substrate and of the additional corrugation is only consistent with adsorption sites *A* and *B*. Theoretical

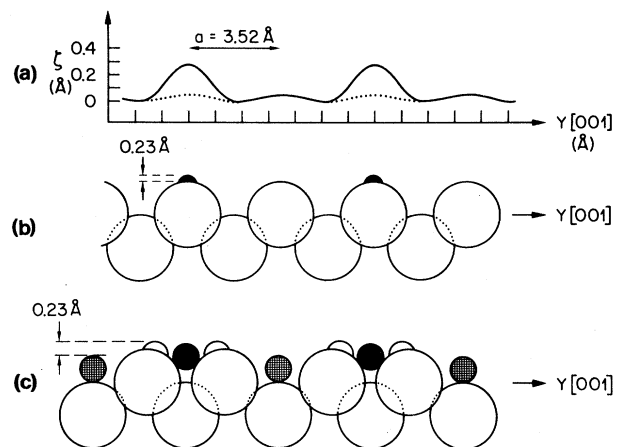


FIG. 3. (a) Best-fit corrugation functions for the clean (dotted line) and hydrogen-saturated (solid line)  $\text{Ni}(110)$  surface; the vertical distances are magnified a factor of 5, relative to the horizontal distances. (b), (c) Hard-sphere models for the  $(1 \times 2)$  structure consistent with the corrugation function shown in (a); the large and small circles designate Ni and H atoms, respectively. (b) Unreconstructed Ni surface, H coverage  $0.5$  [model (a) in the text]. (c) Reconstructed Ni surface [model (c) in the text]; in addition to the positions shown by the shaded circles, H atoms can occupy positions designated by either the full or open circles, corresponding to coverages of  $1.0$  and  $1.5$ , respectively.

calculations<sup>12</sup> have predicted that the *B* sites are preferred. These sites are also occupied by oxygen, whereas sulfur is adsorbed at *C* sites.<sup>13</sup> Figure 3(b) shows a simple hard-wall model consistent with these results. Adsorption on the *B* sites leads to the observed increase in the hard-wall amplitude of  $0.23 \text{ \AA}$  for an H atom with a hard-sphere radius of  $0.4 \text{ \AA}$ . This corresponds to a Ni-H bond length of  $1.65 \text{ \AA}$  in good agreement with the value of  $1.59 \text{ \AA}$  calculated for a site of ligancy 2 on a  $\text{Ni}_{20}$  cluster.<sup>12</sup> This model corresponds to a coverage of  $0.5$ .

One possibility for model (b) is that the nickel rows on which hydrogen is adsorbed are displaced outwards. For this case, the observed corrugation amplitude is a combination of the hard-sphere hydrogen radius and the nickel displacement.

Model (c), shown in Fig. 3(c), has been proposed on the basis of a LEED intensity analysis for  $300\text{-K}$  adsorption.<sup>14</sup> It is consistent with the corrugation function of Fig. 3(a) only if the redistributed charge density gives rise to a subsidiary maximum between the main maxima. In view of the smoothing effect of the valence electrons for the clean surface, this model can explain our

results only if H is adsorbed on both the first and second Ni layers. This structure corresponds to a coverage of 1.0 or 1.5 depending on whether adsorption occurs only on each pair of rows or on each of the paired rows [full and open circles, respectively, in Fig. 3(c)].

It is not possible on the basis of the corrugation function alone to choose unequivocally between the unreconstructed and the two reconstructed models discussed above. It has been proposed that strong additional LEED features upon hydrogen adsorption imply reconstruction,<sup>14</sup> whereas weak features are due to unreconstructed adsorption.<sup>15</sup> We have observed that the He diffraction spectra in Fig. 2 are irreversibly changed upon heating the substrate above 220 K, showing that a reconstruction of the adlayer has taken place. The half-order LEED beams are strong both above and below 220 K which, if used to support reconstruction, requires two distinct reconstructed phases with a transition temperature of 220 K.

We have also observed a  $(2 \times 1)$  He diffraction pattern at lower coverages. The half-order LEED beams of this structure are extremely weak<sup>10</sup> suggesting an unreconstructed surface. A preliminary analysis of our diffraction spectra yields a corrugation amplitude which is similar to that observed for the  $(1 \times 2)$  structure. This indicates that He diffraction, in contrast to LEED, shows a high sensitivity to atomic hydrogen and that the spectra shown in Fig. 2 are primarily due to the charge distribution around the H atoms, rather than to slight shifts in the underlying nickel layers. In view of the higher sensitivity of He diffraction to the charge distribution at the sur-

face, and the higher sensitivity of LEED to the positions of the ion cores in the topmost three to four layers of the solid, the two techniques when applied to the same system can yield valuable complementary information.

The assistance of W. Stocker with the experiments, and of W. Herrmann with the computations, is gratefully acknowledged.

<sup>1</sup>U. Garibaldi, A. C. Levi, R. Spadacini, and G. E. Tommei, *Surf. Sci.* **48**, 649 (1975).

<sup>2</sup>N. Garcia, *J. Chem. Phys.* **67**, 897 (1977).

<sup>3</sup>F. O. Goodman, *J. Chem. Phys.* **66**, 976 (1977).

<sup>4</sup>R. I. Masel, R. P. Merrill, and W. H. Miller, *Phys. Rev. B* **12**, 5545 (1975).

<sup>5</sup>G. Boato, P. Cantini, and L. Mattera, *Surf. Sci.* **55**, 141 (1976).

<sup>6</sup>M. J. Cardillo and G. E. Becker, *Phys. Rev. Lett.* **40**, 1148 (1978).

<sup>7</sup>E. Zaremba and W. Kohn, *Phys. Rev. B* **15**, 1768 (1977).

<sup>8</sup>F. O. Goodman, *Surf. Sci.* **70**, 578 (1978); D. V. Tendulkar and R. E. Stickney, *Surf. Sci.* **27**, 516 (1971).

<sup>9</sup>J. Lapoujouade and K. S. Neil, *J. Chem. Phys.* **70**, 797 (1973).

<sup>10</sup>T. N. Taylor and P. J. Estrup, *J. Vac. Sci. Technol.* **11**, 244 (1974).

<sup>11</sup>K. Christmann, O. Schober, G. Ertl, and M. Neumann, *J. Chem. Phys.* **60**, 4528 (1974).

<sup>12</sup>T. H. Upton and W. A. Goddard, III, *Phys. Rev. Lett.* **42**, 472 (1979).

<sup>13</sup>P. M. Marcus, J. E. Demuth, and D. W. Jepsen, *Surf. Sci.* **53**, 501 (1975).

<sup>14</sup>J. Demuth, *J. Colloid Interface Sci.* **58**, 184 (1977).

<sup>15</sup>M. A. Van Hove, G. Ertl, K. Christmann, R. J. Behm, and W. H. Weinberg, *Solid State Commun.* **28**, 373 (1978).